Scripta Materialia 249 (2024) 116168

Contents lists available at ScienceDirect

Scripta Materialia

journal homepage: www.journals.elsevier.com/scripta-materialia

Shear straining promoted structural transition in bulk metallic glasses

Qifan Wang [a,b], Hongbo Lou [b,c], Dazhe Xu [b], Ziliang Yin [b], Fujun Lan [b], Tao Liang [b], Zilong Zhao [d], Zhaohui Dong [d], Ke Yang [d], Jianrong Zeng [d], Zhidan Zeng [b,c], Qiaoshi Zeng [a,b,c,*]

[a] *Jiangsu Key Laboratory of Advanced Metallic Materials, School of Materials Science and Engineering, Southeast University, Nanjing 211189, China*
[b] *Center for High Pressure Science and Technology Advanced Research, Shanghai 201203, China*
[c] *Shanghai Key Laboratory of Material Frontiers Research in Extreme Environments (MFree), Institute for Shanghai Advanced Research in Physical Sciences (SHARPS), Pudong, Shanghai 201203, China*
[d] *Shanghai Synchrotron Radiation Facility, Shanghai Advanced Research Institute, Chinese Academy of Sciences, Shanghai 201204, China*

ARTICLE INFO

Keywords:
Bulk metallic glass
High pressure
Structural tuning
Synchrotron radiation

ABSTRACT

Metallic glasses (MGs) have unusual structural characteristics and resulting unique properties, but effectively modulating their structure is difficult. The recently achieved two-way structural tuning (ordering-disordering) between distinct states in MGs offers an opportunity to overcome this challenge. However, pressures up to tens of GPa were required for the process, which limits sample sizes at the micrometer scale and challenges further comprehensive research. Here, by introducing concurrent shear straining with compressive force using high-pressure torsion, the pressure to trigger the disordering transition is significantly reduced to a few GPa. This enables the acquisition of millimeter-sized samples for comprehensive study, including synchrotron x-ray diffraction and small angle x-ray scatting, nanoindentation, electrical resistivity, and differential scanning calorimetry. It is evidenced that the two-way tuning of MG can be achieved both structurally and thermodynamically, which could help deepen our understanding of the mechanism behind the two-way tuning and promote exploration of distinct MGs.

Metallic glasses (MGs) have garnered extensive attention owing to their distinctive structural characteristics and resulting superior properties, which distinguish them from conventional crystalline metals or network glasses [1–5]. Despite the lack of well-defined structural models for describing their disordered glass structures, it has been well documented that MGs actually possess pronounced structural features, such as short-range order (SRO) of the nearest-neighbor atoms [6], medium-range order (MRO) on the length scales beyond the nearest neighbor [7–11], or even a long-range topological order (LRTO) throughout a bulk sample [12–14]. In principle, the configurational space for any given MG with multiple components is nearly infinite [15], which suggests vast possibilities for exploring polyamorphous MGs with distinct SRO and or MRO, or even LRTO. Various rejuvenation and relaxation processes are commonly employed aiming at modulating the structure and properties of MGs [16–19], many interesting variations in their atomic structures were reported [20–25]. However, more dramatic structural changes in MGs readily visible by transmission electron microscopy (TEM) or x-ray diffraction (XRD), namely, effective exploration in wider configurational space, is desirable but remains challenging [1, 26].

The recently discovered low-ordering state (LOS) and high-ordering state (HOS) in various MGs including $Ce_{65}Al_{10}Co_{25}$, $La_{65}Al_{10}Co_{25}$, and $Ti_{20}Zr_{20}Hf_{20}Cu_{20}Co_{20}$ MGs with significant differences in their structure factors ($S(q)$) and reduced pair distribution functions ($G(r)$) support the scenario of possibly abundant glass states accessible in the configurational space of MGs [26]. More importantly, a two-way structural tuning between the LOS and HOS has been achieved by simply combining temperature and pressure, offering an effective approach to tuning MGs between distinct states. Specifically, a thermal-driven structural ordering process occurs below the crystallization temperature of the as-quenched MG samples with a well-defined exothermic peak in differential scanning calorimetry (DSC) curves. Nano-scaled density fluctuation was discovered during this ordering transition by synchrotron x-ray small angle scattering (SXAS). Obvious structural changes, especially with enhanced MRO, are also revealed by $S(q)$ and $G(r)$, but without any signature of the long-range crystalline lattice; therefore, the

* Corresponding author at: Jiangsu Key Laboratory of Advanced Metallic Materials, School of Materials Science and Engineering, Southeast University, Nanjing 211189, China.
E-mail address: zengqs@hpstar.ac.cn (Q. Zeng).

https://doi.org/10.1016/j.scriptamat.2024.116168
Received 1 March 2024; Received in revised form 26 April 2024; Accepted 6 May 2024
Available online 9 May 2024

annealed sample is named as HOS, with distinct amorphous structure and density from LOS. Once the HOS is compressed under hydrostatic pressure above a critical value (e.g., 22 GPa for the $Ce_{65}Al_{10}Co_{25}$ MG), the initial LOS seems fully recovered via a reverse disordering transition of the HOS consistently evidenced by *in situ* high-pressure SAXS, $S(q)$, and $G(r)$ data [26].

However, since the pressure required to trigger the disordering transition is pretty high, diamond anvil cells (DACs) are typically used to generate such high pressures. This limitation confines the samples to the micrometer scale, thereby impeding a deeper understanding of its mechanism and potential practical applications of the two-way tuning process. E.g., although the atomic structure of HOS likely transformed back to the initial LOS structure by compression, namely, becoming structurally identical, it remains unclear whether the resultant sample (HP-LOS) is also thermodynamically and or mechanically equivalent to the initial liquid-quenched LOS (LQ-LOS) due to the absence of reliable thermal and mechanical analysis on those tiny samples.

Therefore, reducing the pressure required for the two-way tuning process is crucial to addressing the issues. To achieve this goal, in the present study, a $(La_{0.7}Ce_{0.3})_{65}Al_{10}Co_{25}$ bulk metallic glass (BMG), with enhanced glass forming ability by combining the two MG systems ($Ce_{65}Al_{10}Co_{25}$ and $La_{65}Al_{10}Co_{25}$) [26] with a proper ratio, was chosen as a model BMG system. The HOS $(La_{0.7}Ce_{0.3})_{65}Al_{10}Co_{25}$ BMG can be produced by annealing as expected, confirmed by synchrotron XRD and SAXS measurements. By replacing DACs with a special large-volume press, high-pressure torsion (HPT) apparatus, severe shear (torsional) straining can be introduced during the compression of a millimeter-sized sample [27]. Surprisingly, we find that the HOS bulk sample can transform back to the initial LOS at much lower pressures (4 to 8 GPa) with concurrent shear straining via the HPT process. In contrast, no obvious change occurs with compression alone at identical pressures (no shear straining). With the bulky sample size, the two-way structural tuning products could be readily characterized by DSC, nano-indentation, and electrical resistivity for a detailed comparison between the initial LQ-LOS, annealed HOS, and high-pressure treated HP-LOS.

The master ingots of the $(La_{0.7}Ce_{0.3})_{65}Al_{10}Co_{25}$ alloy were prepared by arc-melting in a Ti-gettered high-purity Ar atmosphere and then cast into rods with a diameter of ~5 mm. Thermal properties were examined using DSC (PerkinElmer DSC 8500) at a heating rate of 20 K/min. The HOS $(La_{0.7}Ce_{0.3})_{65}Al_{10}Co_{25}$ BMG samples were obtained by heating the as-cast LQ-LOS sample to 473 K at a rate of 20 K/min, followed by cooling at 50 K/min to room temperature (denoted as Annealed hereafter). The disc-shaped HOS samples, with a diameter of ~5 mm and a thickness of ~1.1 mm, were subjected to HPT processing at a pressure of ~8 GPa at room temperature plus shear straining with different torsion revolutions (E.g., 20 and 60 revolutions, denoted as A_8GPa20r and as A_8GPa60r, respectively). The HPT process was carried out with a speed of 0.5 rpm to avoid an obvious temperature increase. An additional disc sample was held at 8 GPa for 40 min without rotation (denoted as A_8GPa0r) as a control sample for comparison. The samples after HPT treatment have a thickness of ~600 μm. Since the $(La_{0.7}Ce_{0.3})_{65}Al_{10}Co_{25}$ BMG is much softer than the typical Zr-based or Pd-based BMGs studied by HPT, significant macroscopic spatial heterogeneity as reported before [28] is not expected along the radial direction with high torsion revolutions (as evidenced by Supplementary Fig. 1S). However, to keep experimental results more consistent, all measurements on the HPT-treated samples were carried out at the similar positions of the samples (a near-edge part with a square shape of 2 mm × 2 mm. The square center is 1 mm from the edge and 1.5 mm from the center of the HPT-treated samples). Nanoindentation tests were performed using an instrumented nano Indenter (G200, Keysight, USA) equipped with a standard Berkovich diamond indenter under a displacement-control mode using a maximum load of 30 mN and a loading rate of 2 mN/s at room temperature. Sample surfaces were carefully ground and polished to a mirror finish before each nanoindentation test. A total of 16 indents (a 4 × 4 array with the interval of 50 μm) were measured for each sample for averaging. Electrical resistivity measurements were carried out using a standard four-probe method with a direct current of 5 mA. Synchrotron SAXS measurements were conducted at the beamline BL40XU, SPring-8, Japan, with an x-ray energy of 15 keV and a beam size of 50 × 50 μm. High-energy synchrotron XRD experiments were performed at the beamline BL12SW, Shanghai Synchrotron Radiation Facility, China, with an x-ray energy of 88.4 keV and a beam size of 0.5 × 0.5 mm.

Fig. 1a shows the DSC curves of the $(La_{0.7}Ce_{0.3})_{65}Al_{10}Co_{25}$ BMGs at different glass states. The as-cast sample undergoes an obvious exothermic relaxation below the glass transition temperature, T_g ~443.5 K. The first sharp exothermic peak, which corresponds to a structural ordering transition [26], starts at ~455 K and ends at ~498 K, and the integral area of the exothermic peak is ~14.4 J/g, followed by crystallization peaks above ~534 K. After annealing the as-cast sample at ~473 K, it transforms to an HOS glass and the initial first sharp exothermic peak disappears and T_g increases significantly to ~451.8 K. In contrast, the following crystallization peaks remain intact, which is consistent with the previous observations in similar MG systems, e.g., $Ce_{65}Al_{10}Co_{25}$ and $La_{65}Al_{10}Co_{25}$ MGs [26] and $(La_{0.5}Ce_{0.5})_{65}Al_{10}Co_{25}$ MGs [29]. No obvious alteration can be observed in the DSC curve after compressing the HOS sample at 8 GPa without torsion using the HPT apparatus. This is consistent with previous study that HOS samples subjected to high-pressure treatment in DACs typically require pressures above 22 GPa to trigger the structural disordering transition [26]. In contrast, when additional torsional straining is involved, i.e., rotating by 20 revolutions at 8 GPa, the first exothermic peak is partially recovered by a peak area of 8.6 J/g (~6 0% of the initial exothermic peak area) in the DSC curves. By further increasing the revolution to 60, the exothermic peak area increases correspondingly to 13.1 J/g, which is very close to that of the initial LQ-LOS samples (Fig. 1c), achieving a significant recovery of enthalpy by mechanical treatment of MGs. Such enormous enthalpy recovery suggests a significant alteration in glassy structures and property. This result demonstrates that severe shear straining could dramatically accelerate the disordering transition in this BMG and could mechanically bring the HOS BMG back to its initial liquid-quenched glass state. Additional experiments with lower pressure but identical torsion revolutions confirm both pressure and shear straining could facilitate the disordering transition (Supplementary Fig. S2). In the A_8GPa60r sample, the glass transition becomes obvious and the T_g (~441.5 K) is also almost identical to that of the as-cast LQ-LOS sample, which confirms the glass nature of the HPT-LOS as a thermodynamic equivalent of the LQ-LOS.

The corresponding reduced pair distribution functions, $G(r)$, of the samples, are shown in Fig. 1b. Similar to the two-way tuning between the LOS and HOS structures observed in the $Ce_{65}Al_{10}Co_{25}$ MG [26], the thermal-induced ordering and HPT-induced disordering is well demonstrated in $G(r)$. It is worth noting that simply compressing the HOS sample at 8 GPa is not sufficient to trigger the disordering transition, which can be seen from its almost intact DSC and $G(r)$ data compared with those of the annealed HOS sample. However, by introducing shear straining in addition to the 8 GPa compression, both the structure and enthalpy are almost fully recovered to the initial LQ-LOS state (even more rejuvenated according to the larger relaxation exotherm below T_g), see the comparison of the as-cast and A_8GPa60r data in Figs. 1c and 1d. At the nanoscale, the HOS samples usually show characteristic density fluctuations [26]. The synchrotron SAXS measurements (Fig. 2) also confirm the structural feature of the density fluctuation in the HOS $(La_{0.7}Ce_{0.3})_{65}Al_{10}Co_{25}$ BMG. The prominent hump centered at ~0.04 $\mathring{A}^{-1}$ was observed after annealing and subsequently suppressed by HPT treatment, which demonstrate that this density fluctuation can be effectively removed by HPT with torsion at a much lower pressure (8 GPa) compared with the pure hydrostatic pressure up to 22 GPa required in the $Ce_{65}Al_{10}Co_{25}$ MG using DACs [26].

Due to the relatively low pressure, the samples for HPT processing can be millimeter- or centimeter-sized in diameter. Therefore, almost all

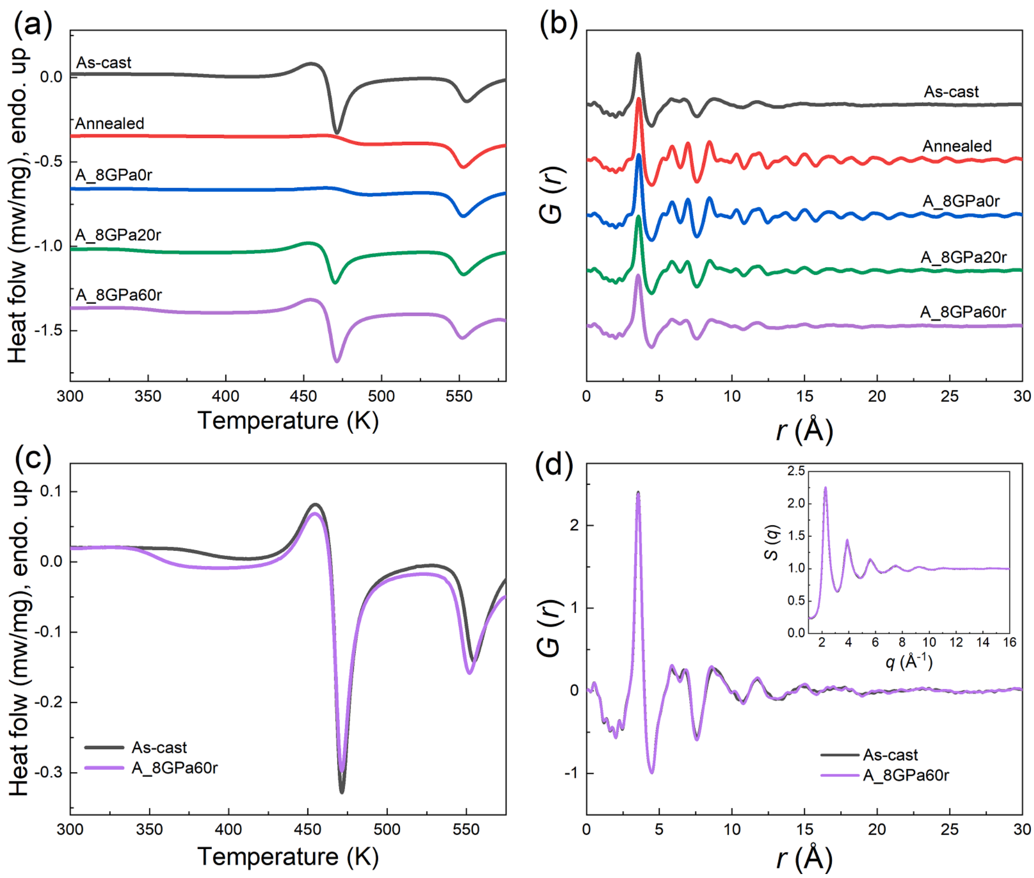

Fig. 1. (a) The DSC curves of the as-cast, annealed and HPT treated $(La_{0.7}Ce_{0.3})_{65}Al_{10}Co_{25}$ BMGs. (b) $G(r)$ of the samples after different processing. Comparison of the DSC curves (c) and $G(r)$ and $S(q)$ (d) between the as-cast and A-8GPa60r samples.

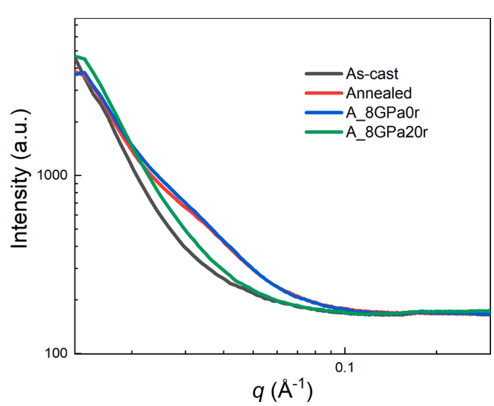

Fig. 2. SAXS results of the $(La_{0.7}Ce_{0.3})_{65}Al_{10}Co_{25}$ BMGs with different states.

typical characterization methods can be readily employed for the HPT-processed BMG samples, which is a major advantage compared with the micrometer-sized samples obtained by DACs. The mechanical properties were measured by nanoindentation tests for the $(La_{0.7}Ce_{0.3})_{65}Al_{10}Co_{25}$ BMG samples with different states. Compared with the LQ-LOS sample, both the hardness and Young's modulus increase substantially after annealing (HOS), and these values remain almost unchanged after compression at 8 GPa (A_8GPa0r), as shown in Fig. 3a, which confirms the neglectable effect of compressive pressure of 8 GPa alone. However, as long as shear straining is introduced with pressure, the hardness and modulus of the annealed samples are significantly reduced. In addition, as shown in Supplementary Fig.S3, the A_4GPa20r sample, obviously rejuvenated but mostly remaining HOS after HPT treatment, exhibits only minimal changes in properties, implying that the structural transition between distinct glass states exerts a more significant influence on the properties modulating compared with the conventional deformation-induced rejuvenation effect [11]. Therefore, compared with the initial LQ-LOS sample, the slightly smaller hardness and Young's modulus observed in the HPT-HOS sample could be mainly attributed to their higher energy states achieved (rejuvenated) after HPT indicated by the larger relaxation exotherm before T_g, as shown in Fig. 1c.

As a sensitive property to structural order in MGs, electrical resistivity was determined on the different $(La_{0.7}Ce_{0.3})_{65}Al_{10}Co_{25}$ BMG samples. The electrical resistivity of the as-cast $(La_{0.7}Ce_{0.3})_{65}Al_{10}Co_{25}$ BMG is determined to be ~180 μΩ·cm at room temperature, close to the typical values of La-based MGs in other studies [30,31]. The resistivity significantly decreases after annealing in HOS. After further compression at 8 GPa without shear straining of the HOS sample, the resistivity remains nearly constant. In contrast, pronounced recovery of the resistivity is obtained after compression at 8 GPa with additional shear straining using HPT, and eventually returns to almost the same value of the LQ-LOS sample when the torsion revolutions are increased to 60, aligning well with the variations of the structure and enthalpy.

The pressure-sensitive 4*f* electrons have been reported to account for many interesting polyamorphic transitions in MGs under pressure [32–34]. To address the possible 4*f* electron effect on the reported shear straining accelerated structural disordering transition in this work, the $La_{65}Al_{10}Co_{25}$ MG samples without 4*f* electrons but with reported LOS and HOS [26,29,35] were further investigated. Fig. 4a shows a similar recovery of the ordering peak in the DSC curves after HPT treatment on the HOS $La_{65}Al_{10}Co_{25}$ MG samples, which rules out a dramatic 4*f* electron effect.

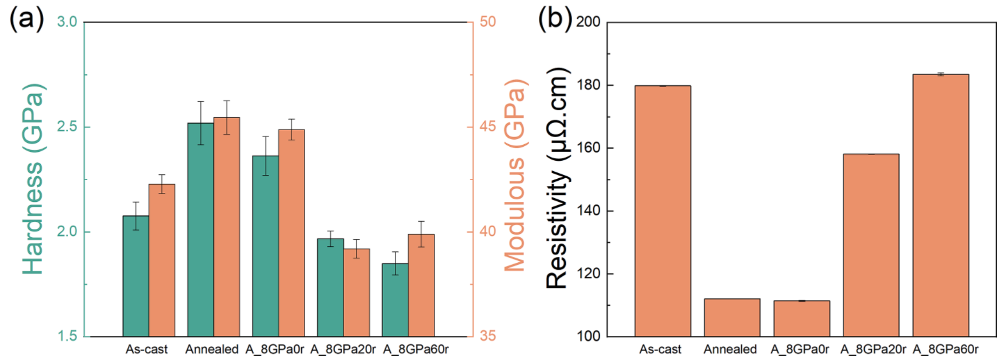

Fig. 3. Property measurements of the $(La_{0.7}Ce_{0.3})_{65}Al_{10}Co_{25}$ BMGs. (a) The comparison of hardness and Young's modulus. The error bars represent the fluctuation among the 16 different measurements on each sample. (b) Electrical resistivity of the different samples.

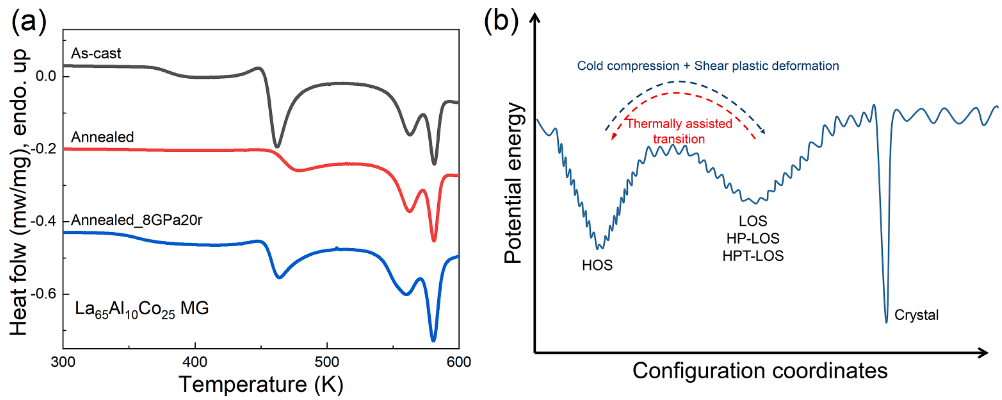

Fig. 4. (a) DSC curves of the as-prepared and annealed and subsequent HPT-treated $La_{65}Al_{10}Co_{25}$ MG sample, showing the ordering and disordering transitions. The first exothermic peak (ordering peak) disappearing after annealing restores obviously after 20 revolutions of HPT at 8 GPa. (b) Schematic diagram of the potential energy landscape. The x-axis represents configuration coordinates. The three states labeled LOS/HP-LOS/HPT-LOS, HOS, and crystal differ in the shape and depth of their potential energy well/megabasins. The thermal-driven transition from LOS to HOS and the pressure-deformation-driven transition from HOS back to LOS (HP-LOS/HPT-LOS) are indicated by the red and blue dashed arrows, respectively. Please note that the real PEL may be very complex and the transition path between different states is not necessarily limited in the plane of the paper.

For crystalline materials, it is well known that plastic deformation may induce lattice defects such as vacancies, dislocations, grain boundaries, etc., often accompanied by an increase in hardness and also could affect the kinetics of phase transitions by changing the mobility of atoms and or free energy landscape of a material [27,36,37]. Many of BMGs are brittle at room temperature. Therefore, HPT is an effective technique to achieve severe plastic deformation for those BMGs by providing confining compressive force and concurrent torsional straining. Previous studies have demonstrated that HPT treatment could induce short-range atomic rearrangement of MGs and structural rejuvenation mainly associated with forming shear bands [38–47], and sometimes even destabilizes MGs with nano-crystallization [48,49]. However, the effect of shear stress/strain on polyamorphic transitions in MGs has not been explored before. Although the detailed mechanism remains unclear, the observations in this work underscore the critical role of shear straining in atomic structural stability/transition in MGs. Moreover, the acceleration of the HOS to LOS transition by shear straining resembles the classical martensitic transitions in crystalline materials, suggesting a possible displacive nature of the transition.

Previously, it has been demonstrated that two-way tuning could be realized in various MGs by combining temperature and pressure [26]. However, as one dimensional averaged structural information, the almost identical $S(q)$ and $G(r)$ could not lead to conclude whether the initial LQ-LOS glass is really retrieved or not. Fortunately, in this work, for the first time, the HPT-LOS sample is evidenced to be thermodynamically similar to the LQ-LOS sample. By employing the potential energy landscape (PEL) diagram [50], as shown in Fig. 4b, what we achieved in this work can be more easily illustrated. Shear stress/-straining may change the energy landscape with enhanced glass dynamics [51] and facilitate the HOS to LOS transition. Since HPT-LOS is intrinsically similar to LQ-LOS in terms of atomic structure and enthalpy, they should locate in the same energy megabasin, realizing a shear-straining accelerated two-way tuning of glasses at relatively low pressures.

In conclusion, through a comprehensive study on MGs with thermal-assisted formation of HOS, it is revealed that the annealed HOS BMG can transform into an HPT-LOS by HPT processing at much lower pressures than previous hydrostatic compression studies once severe shear straining is involved. The obtained HPT-LOS is confirmed to be not only structurally but also thermodynamically similar to the LQ-LOS, which suggests that the mechanical processing route far below T_g could be equivalent to the traditional route through liquid quenching for glass formation [52]. These findings offer an effective approach to the exploration of distinct MG states freely in the configurational space, overcoming the natural one-way trend of aging. Furthermore, the unique role of shear straining underscored in this work, along with its interaction with pressure and temperature in MGs formation [53] and transformation, warrants further studies utilizing MGs with the HOS to LOS transitions as model systems.

Data availability

Data will be made available on request.

CRediT authorship contribution statement

Qifan Wang: Writing – original draft, Validation, Methodology, Investigation, Formal analysis, Data curation. **Hongbo Lou:** Writing – review & editing, Validation, Supervision, Investigation, Formal analysis, Data curation. **Dazhe Xu:** Investigation, Formal analysis. **Ziliang Yin:** Investigation. **Fujun Lan:** Investigation. **Tao Liang:** Investigation. **Zilong Zhao:** Investigation. **Zhaohui Dong:** Investigation. **Ke Yang:** Supervision, Resources. **Jianrong Zeng:** Supervision, Resources. **Zhidan Zeng:** Validation, Supervision, Project administration, Formal analysis. **Qiaoshi Zeng:** Writing – review & editing, Validation, Supervision, Resources, Project administration, Methodology, Funding acquisition, Formal analysis, Conceptualization.

Declaration of competing interest

The authors declare that they have no known competing financial interests or personal relationships that could have appeared to influence the work reported in this paper.

Acknowledgments

The authors acknowledge financial support from Shanghai Key Laboratory of Material Frontiers Research in Extreme Environments, China (No. 22dz2260800), the Shanghai Science and Technology Committee, China (No. 22JC1410300), and the National Natural Science Foundation of China (No. 52101187). SAXS measurements were conducted at the beamline BL40XU, SPring-8, Japan, with the great help and support of Dr. Hiroshi Sekiguchi and Dr. Koki Aoyama. High-energy synchrotron XRD experiments were performed mainly at the beamline 12SW and partially at the beamline 13SSW, Shanghai Synchrotron Radiation Facility, China, with the kind help from Dr. Hongliang Dong.

Supplementary materials

Supplementary material associated with this article can be found, in the online version, at doi:10.1016/j.scriptamat.2024.116168.

References

[1] E. Ma, Tuning order in disorder, Nat. Mater. 14 (6) (2015) 547–552.
[2] W.L. Johnson, Bulk glass-forming metallic alloys: science and technology, MRS Bull. 24 (10) (1999) 42–56.
[3] A. Inoue, A. Takeuchi, Recent development and application products of bulk glassy alloys, Acta Mater. 59 (6) (2011) 2243–2267.
[4] W.H. Wang, Bulk metallic glasses with functional physical properties, Adv. Mater. 21 (45) (2009) 4524–4544.
[5] A.L. Greer, E. Ma, Bulk metallic glasses: at the cutting edge of metals research, MRS Bull. 32 (8) (2007) 611–619.
[6] A. Hirata, P. Guan, T. Fujita, Y. Hirotsu, A. Inoue, A.R. Yavari, T. Sakurai, M. Chen, Direct observation of local atomic order in a metallic glass, Nat. Mater. 10 (1) (2011) 28–33.
[7] H.W. Sheng, W.K. Luo, F.M. Alamgir, J.M. Bai, E. Ma, Atomic packing and short-to-medium-range order in metallic glasses, Nature 439 (7075) (2006) 419–425.
[8] D.B. Miracle, A structural model for metallic glasses, Nat. Mater. 3 (10) (2004) 697–702.
[9] X.W. Fang, C.Z. Wang, S.G. Hao, M.J. Kramer, Y.X. Yao, M.I. Mendelev, Z.J. Ding, R.E. Napolitano, K.M. Ho, Spatially resolved distribution function and the medium-range order in metallic liquid and glass, Sci. Rep. 1 (1) (2011) 194.
[10] T. Egami, C.W. Ryu, World beyond the nearest neighbors, J. Phys. Condens. Matter 35 (17) (2023) 174002.
[11] S. Lan, L. Zhu, Z. Wu, L. Gu, Q. Zhang, H. Kong, J. Liu, R. Song, S. Liu, G. Sha, Y. Wang, Q. Liu, W. Liu, P. Wang, C.T. Liu, Y. Ren, X.L. Wang, A medium-range structure motif linking amorphous and crystalline states, Nat. Mater. 20 (10) (2021) 1347–1352.
[12] Q. Zeng, H. Sheng, Y. Ding, L. Wang, W. Yang, J.Z. Jiang, W.L. Mao, H.K. Mao, Long-range topological order in metallic glass, Science 332 (6036) (2011) 1404–1406.
[13] D. Ma, A.D. Stoica, X.L. Wang, Power-law scaling and fractal nature of medium-range order in metallic glasses, Nat. Mater. 8 (1) (2009) 30–34.
[14] C.W. Ryu, W. Dmowski, K.F. Kelton, G.W. Lee, E.S. Park, J.R. Morris, T. Egami, Curie-Weiss behavior of liquid structure and ideal glass state, Sci. Rep. 9 (1) (2019) 18579.
[15] F.H. Stillinger, A topographic view of supercooled liquids and glass formation, Science 267 (5206) (1995) 1935–1939.
[16] Y. Sun, A. Concustell, A.L. Greer, Thermomechanical processing of metallic glasses: extending the range of the glassy state, Nat. Rev. Mater. 1 (9) (2016) 16039.
[17] J. Pan, Y.X. Wang, Q. Guo, D. Zhang, A.L. Greer, Y. Li, Extreme rejuvenation and softening in a bulk metallic glass, Nat. Commun. 9 (1) (2018) 560.
[18] J. Pan, Y.P. Ivanov, W.H. Zhou, Y. Li, A.L. Greer, Strain-hardening and suppression of shear-banding in rejuvenated bulk metallic glass, Nature 578 (7796) (2020) 559–562.
[19] S.V. Ketov, Y.H. Sun, S. Nachum, Z. Lu, A. Checchi, A.R. Beraldin, H.Y. Bai, W. H. Wang, D.V. Louzguine-Luzgin, M.A. Carpenter, A.L. Greer, Rejuvenation of metallic glasses by non-affine thermal strain, Nature 524 (7564) (2015) 200–203.
[20] J. Hwang, Z.H. Melgarejo, Y.E. Kalay, I. Kalay, M.J. Kramer, D.S. Stone, P. M. Voyles, Nanoscale structure and structural relaxation in Zr50Cu45Al5 bulk metallic glass, Phys. Rev. Lett. 108 (19) (2012) 195505.
[21] S. Hilke, H. Rösner, D. Geissler, A. Gebert, M. Peterlechner, G. Wilde, The influence of deformation on the medium-range order of a Zr-based bulk metallic glass characterized by variable resolution fluctuation electron microscopy, Acta Mater. 171 (2019) 275–281.
[22] F.A. Davani, S. Hilke, H. Rösner, D. Geissler, A. Gebert, G. Wilde, Correlations between the ductility and medium-range order of bulk metallic glasses, J. Appl. Phys. 128 (1) (2020) 015103.
[23] A. Hassanpour, S. Hilke, H. Rösner, S.V. Divinski, G. Wilde, Impact of severe plastic deformation on the relaxation of glassy and supercooled liquid states of amorphous Pd40Ni40P20, J. Appl. Phys. 128 (15) (2020) 155107.
[24] K. Nomoto, A.V. Ceguerra, C. Gammer, B. Li, H. Bilal, A. Hohenwarter, B. Gludovatz, J. Eckert, S.P. Ringer, J.J. Kruzic, Medium-range order dictates local hardness in bulk metallic glasses, Mater. Today 44 (2021) 48–57.
[25] K. Nomoto, B. Li, C. Gammer, A.V. Ceguerra, H. Bilal, A. Hohenwarter, J. Eckert, B. Gludovatz, S.P. Ringer, J.J. Kruzic, Deformation-induced medium-range order changes in bulk metallic glasses, Phys. Rev. Mater. 6 (4) (2022) 043603.
[26] H. Lou, Z. Zeng, F. Zhang, S. Chen, P. Luo, X. Chen, Y. Ren, V.B. Prakapenka, C. Prescher, X. Zuo, T. Li, J. Wen, W.H. Wang, H. Sheng, Q. Zeng, Two-way tuning of structural order in metallic glasses, Nat. Commun. 11 (1) (2020) 314.
[27] A.P. Zhilyaev, T.G. Langdon, Using high-pressure torsion for metal processing: fundamentals and applications, Prog. Mater. Sci. 53 (6) (2008) 893–979.
[28] W. Zhao, H. Cheng, X. Jiang, M.L. Wu, G. Li, Effect of destined high-pressure torsion on the structure and mechanical properties of rare earth-based metallic glasses, Metall. Mater. Trans. A 49 (3) (2018) 842–847.
[29] J. Shen, Z. Lu, J. Wang, S. Lan, F. Zhang, A. Hirata, M. Chen, X.L. Wang, P. Wen, Y. H. Sun, H.Y. Bai, W. Wang, Metallic glacial glass formation by a first-order liquid-liquid transition, J. Phys. Chem. Lett. (2020).
[30] Q.S. Zeng, Y.C. Li, C.M. Feng, P. Liermann, M. Somayazulu, G.Y. Shen, H.k. Mao, R. Yang, J. Liu, T.D. Hu, J.Z. Jiang, Anomalous compression behavior in lanthanum/cerium-based metallic glass under high pressure, Proc. Natl. Acad. Sci. 104 (34) (2007) 13565–13568.
[31] B.Y. Liu, F. Ye, Glass transition kinetics of La55Al25Ni10Cu10 bulk metallic glass by electrical resistivity measurement, Rare Met. 32 (4) (2013) 359–362.
[32] Q.S. Zeng, Y. Ding, W.L. Mao, W. Yang, S.V. Sinogeikin, J. Shu, H.K. Mao, J. Z. Jiang, Origin of pressure-induced polyamorphism in Ce75Al25 metallic glass, Phys. Rev. Lett. 104 (10) (2010) 105702.
[33] Q.S. Zeng, Y.C. Li, C.M. Feng, P. Liermann, M. Somayazulu, G.Y. Shen, H.K. Mao, R. Yang, J. Liu, T.D. Hu, J.Z. Jiang, Anomalous compression behavior in lanthanum/cerium-based metallic glass under high pressure, Proc. Natl. Acad. Sci. U. S. A. 104 (34) (2007) 13565–13568.
[34] H.W. Sheng, H.Z. Liu, Y.Q. Cheng, J. Wen, P.L. Lee, W.K. Luo, S.D. Shastri, E. Ma, Polyamorphism in a metallic glass, Nat. Mater. 6 (3) (2007) 192–197.
[35] Q. Yang, S. Wei, Y. Yu, H.R. Zhang, L. Gao, Q.Z. Bu, N. Amini, Y.D. Cheng, F. Yang, A. Schoekel, H.B. Yu, Structural length-scale of β relaxation in metallic glass, J. Chem. Phys. 157 (18) (2022).
[36] R. Pippan, S. Scheriau, A. Taylor, M. Hafok, A. Hohenwarter, A. Bachmaier, Saturation of fragmentation during severe plastic deformation, Annu. Rev. Mater. Res. 40 (1) (2010) 319–343.
[37] D. Rodney, L. Proville, Stress-dependent Peierls potential: influence on kink-pair activation, Phys. Rev. B 79 (9) (2009) 094108.
[38] W. Dmowski, Y. Yokoyama, A. Chuang, Y. Ren, M. Umemoto, K. Tsuchiya, A. Inoue, T. Egami, Structural rejuvenation in a bulk metallic glass induced by severe plastic deformation, Acta Mater. 58 (2) (2010) 429–438.
[39] F. Meng, K. Tsuchiya, Seiichiro II, Y. Yokoyama, Reversible transition of deformation mode by structural rejuvenation and relaxation in bulk metallic glass, Appl. Phys. Lett. 101 (12) (2012) 121914.
[40] H. Zhou, S. Hilke, E. Pineda, M. Peterlechner, Y. Chushkin, S. Shanmugam, G. Wilde, X-ray photon correlation spectroscopy revealing the change of relaxation dynamics of a severely deformed Pd-based bulk metallic glass, Acta Mater. 195 (2020) 446–453.
[41] H. Zhou, M. Peterlechner, S. Hilke, D. Shen, G. Wilde, Influence of plastic deformation by high-pressure torsion on the crystallization kinetics of a Pd40Ni40P20 bulk metallic glass, J. Alloys Compd. 821 (2020) 153254.
[42] C. Ebner, B. Escher, C. Gammer, J. Eckert, S. Pauly, C. Rentenberger, Structural and mechanical characterization of heterogeneities in a CuZr-based bulk metallic glass processed by high pressure torsion, Acta Mater. 160 (2018) 147–157.
[43] X.L. Bian, D. Zhao, J.T. Kim, D. Şopu, G. Wang, R. Pippan, J. Eckert, Controlling the distribution of structural heterogeneities in severely deformed metallic glass, Mater. Sci. Eng. A 752 (2019) 36–42.

[44] H. Zhou, R. Hubek, M. Peterlechner, G. Wilde, Two-stage rejuvenation and the correlation between rejuvenation behavior and the boson heat capacity peak of a bulk metallic glass, Acta Mater. 179 (2019) 308–316.
[45] F. Meng, K. Tsuchiya, M.J. Kramer, R.T. Ott, Reduction of shear localization through structural rejuvenation in Zr–Cu–Al bulk metallic glass, Mater. Sci. Eng. A 765 (2019) 138304.
[46] D.V. Gunderov, A.A. Churakova, E.V. Boltynjuk, E.V. Ubyivovk, V.V. Astanin, R. N. Asfandiyarov, R.Z. Valiev, W. Xioang, J.T. Wang, Observation of shear bands in the Vitreloy metallic glass subjected to HPT processing, J. Alloys Compd. 800 (2019) 58–63.
[47] P. Denis, C.M. Meylan, C. Ebner, A.L. Greer, M. Zehetbauer, H.J. Fecht, Rejuvenation decreases shear band sliding velocity in Pt-based metallic glasses, Mater. Sci. Eng. A 684 (2017) 517–523.
[48] Z.Q. Ren, A.A. Churakova, X. Wang, S. Goel, S.N. Liu, Z.S. You, Y. Liu, S. Lan, D. V. Gunderov, J.T. Wang, R.Z. Valiev, Enhanced tensile strength and ductility of bulk metallic glasses Zr52.5Cu17.9Al10Ni14.6Ti5 via high-pressure torsion, Mater. Sci. Eng. A 803 (2021) 140485.
[49] Y. Dong, S. Liu, J. Biskupek, Q. Cao, X. Wang, J.Z. Jiang, R. Wunderlich, H.J. Fecht, Improved tensile ductility by severe plastic deformation for nano-structured metallic glass, Materials (2019) (Basel).
[50] F.H. Stillinger, A topographic view of supercooled liquids and glass formation, Science 267 (5206) (1995) 1935–1939.
[51] C. Liu, Y. Fan, Emergent fractal energy landscape as the origin of stress-accelerated dynamics in amorphous solids, Phys. Rev. Lett. 127 (21) (2021) 215502.
[52] J. Ketkaew, W. Chen, H. Wang, A. Datye, M. Fan, G. Pereira, U.D. Schwarz, Z. Liu, R. Yamada, W. Dmowski, M.D. Shattuck, C.S. O'Hern, T. Egami, E. Bouchbinder, J. Schroers, Mechanical glass transition revealed by the fracture toughness of metallic glasses, Nat. Commun. 9 (1) (2018) 3271.
[53] P. Guan, M. Chen, T. Egami, Stress-temperature scaling for steady-state flow in metallic glasses, Phys. Rev. Lett. 104 (20) (2010) 205701.